

PAPER • OPEN ACCESS

Quantitative analysis of $\{100\}_{\text{Al}}$ plate/lath- and $\langle 100 \rangle_{\text{Al}}$ rod-shaped precipitates in an aged Al-Cu-Mg-Si alloy using TEM

To cite this article: M R Gazizov *et al* 2021 *IOP Conf. Ser.: Mater. Sci. Eng.* **1014** 012013

View the [article online](#) for updates and enhancements.

You may also like

- [Discoloration of Anodized AA6063 Aluminum Alloy](#)
Y. Ma, X. Zhou, J. Wang *et al.*
- [Design and development of laser speckle reduction device using waveguide diffuser and pyramidal cavity for projection imaging](#)
Virendra Kumar, Mayank Gupta, Atul Kumar Dubey *et al.*
- [Synthesis and evaluation of nano -Al₂O₃ with spherical, rod-shaped, and plate-like morphologies on enhanced heavy oil recovery](#)
Rasool Rasooli Manesh, Mohammad Kohnehpoushi, Mehdi Eskandari *et al.*



The Electrochemical Society
Advancing solid state & electrochemical science & technology

242nd ECS Meeting

Oct 9 – 13, 2022 • Atlanta, GA, US

Abstract submission deadline: **April 8, 2022**

Connect. Engage. Champion. Empower. Accelerate.

MOVE SCIENCE FORWARD



Submit your abstract



Quantitative analysis of $\{100\}_{\text{Al}}$ plate/lath- and $\langle 100 \rangle_{\text{Al}}$ rod-shaped precipitates in an aged Al-Cu-Mg-Si alloy using TEM

M R Gazizov^{1,*}, R Holmestad², C D Marioara³ and R O Kaibyshev¹

¹Belgorod State University, Pobeda, 85, Belgorod, 308015, Russia

²Department of Physics, Norwegian University Science and Technology (NTNU), Trondheim, 7491, Norway

³Materials and Nanotechnology, SINTEF Industry, Trondheim, 7465, Norway

*Corresponding author: gazizov@bsu.edu.ru

Abstract. Precipitate parameters, such as length, diameter and thickness of rationally oriented $\{100\}_{\text{Al}}$ plate/lath-shaped and $\langle 100 \rangle_{\text{Al}}$ rod-shaped precipitates in an age-hardenable Al-Cu-Mg-Si alloy have been examined quantitatively. An appropriate procedure of the plate- and rod-shaped precipitate separation was suggested to determine the precipitate parameters as well as their distribution histograms using bright- (BF) and dark-field (DF) transmission electron microscopy (TEM) images taken in the $\langle 100 \rangle_{\text{Al}}$ and $\langle 110 \rangle_{\text{Al}}$ zone axes (ZA).

1. Introduction

The size and morphology of precipitates are important parameters of the microstructure of age-hardenable aluminium alloys, because they determine their service properties of these materials. In the case of Al-Cu-Mg-Si alloys, the presence of rationally oriented plate- or/and lath-shaped precipitates with $\{100\}_{\text{Al}}$ habit planes and rod-shaped precipitates along the $\langle 100 \rangle_{\text{Al}}$ direction consisting of diverse phase fragments takes place after aging [1,2]. Quantitative characterization of several types of precipitates has not been performed, despite this may help to better understand the effect of various thermomechanical parameters (temperature, time, strain, etc.) on the microstructure of precipitates in these alloys, as well as to estimate the precipitate strengthening contribution to the strength of the material.

Different analytical techniques can be used to characterize the precipitation behaviour [3,4]. However, conventional TEM [5,6] still remains an attractive technique because this method is relatively fast and provides direct observations of the precipitates to measure their sizes and analyze their distribution although it may give poorer statistics. The major drawback of different TEM techniques is that the output is 2D projection images, which may be difficult to interpret in 3D. In the Al-Cu-Mg-Si alloys, TEM images taken along different ZA do not allow to identify and separate rationally oriented $\{100\}_{\text{Al}}$ plates and $\langle 100 \rangle_{\text{Al}}$ rods because these projected precipitates look similarly in representative TEM images. The aim of the present work has been to develop an appropriate procedure for quantitative characterization of precipitate parameters such as size, number density and volume fraction in an Al-Cu-Mg-Si alloy using conventional TEM.



2. Materials and methods

An aluminum alloy with the chemical composition of Al-4.9Cu-0.74Mg-0.51Si-0.48Mn-0.1Cr-0.08Ti-0.02Fe (wt. %) was cast and subjected to thermomechanical treatment (TMT) as described in [1,2]. It should be just noted final TMT steps included solution heat treatment at 500 °C for 1 h followed by water-quenching to room temperature and then aging at 170 °C in the time range up to 96 hours [1].

Details of the sample preparation procedure for TEM analysis are given in [1,2]. TEM analysis was performed on JEOL JEM-2100 and JEM-2100F microscopes operated at 200 kV. Observations were carried out with an electron beam parallel to an $\langle 100 \rangle_{\text{Al}}$ and $\langle 110 \rangle_{\text{Al}}$ ZA with DF images using $\vec{g} = 110_{\text{Al}}$ and 100_{Al} , respectively. Foil thickness (ϕ) was measured by convergent beam electron diffraction (CBED) [6]. All the precipitate parameters were estimated taking the tilting of the TEM foils into account. The Crystal Studio V10 software was used to simulate different diffraction patterns (DPs) including spots of the first-, second- and third-order Laue zones. This simulation condition did not take into account double diffraction. The procedure of ZA calculation for the lattices of the precipitates, having orientation relationships (ORs), in the respective $\{100\}_{\text{Al}}$ and $\{110\}_{\text{Al}}$ projections was described in [9]. The simulated DPs were validated for the β'' - and θ' -phases in the Al matrix by [9] and [10], respectively.

3. Results and Discussions

TEM images, showing a typical precipitate microstructure in the Al-Cu-Mg-Si alloy aged for 16 and 96 h, are given in figure 1a-b. A close examination reveals the presence of two precipitate groups categorized by morphology in the images taken along $\langle 100 \rangle_{\text{Al}}$ and $\langle 110 \rangle_{\text{Al}}$ ZA. The first group is associated with $\langle 100 \rangle_{\text{Al}}$ rod-shaped precipitates normal to the image and clearly seen in cross-section in the $\{100\}_{\text{Al}}$ projections as dark and bright dots in the BF and DF images, respectively (marked as a_1 in figure 1a). These precipitates are of a hybrid type consisting of small fragments of the β'' , β' -Cu, C and Q' phases, sometimes forming somewhat jagged bands along dislocation lines [1]. Some of these rods having in-plane orientation appear as elongated 'rectangles' marked by a_2 in figure 1a. However, a certain fraction of these elongated 'rectangles' are caused by projections of plate- or lath-shaped particles categorized as the second group of precipitates. These precipitates can be identified as discrete C laths and θ' plates with $\{100\}_{\text{Al}}$ habit planes. They are clearly seen in DF-TEM images taken along $\langle 110 \rangle_{\text{Al}}$ ZA using an aperture in the forbidden $\vec{g}=001_{\text{Al}}$ position (figure 1b).

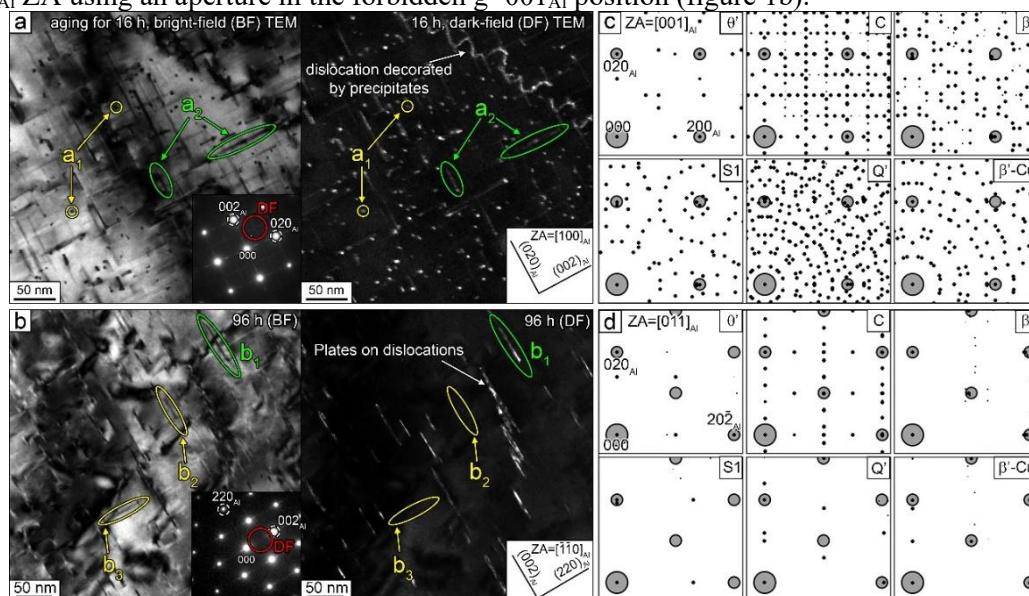


Figure 1. BF and DF-TEM images of the typical microstructure in an Al-Cu-Mg-Si alloy aged for 16 h (a) and 96 h (b); Superposition of simulated DPs for the Al matrix in $\langle 100 \rangle_{\text{Al}}$ ZA (c) and $\langle 110 \rangle_{\text{Al}}$ ZA (d) and for the precipitates with ORs from [1,2,4]. ZAs for the precipitates were determined using a method in [9].

DP simulations, performed for the β'' -, β' -Cu, C-, Q'-, S1 and θ' -phases previously found in the same Al-Cu-Mg-Si alloy and having respective ORs, are presented in figure 1d and e. The DPs for these phases were obtained for the directions corresponding to the $\langle 100 \rangle_{\text{Al}}$ and $\langle 110 \rangle_{\text{Al}}$ ZA. It is seen in figure 1b and c that DPs for the AlMgSi(Cu) phases (β'' -, β' -Cu, C- and Q'-phase) show a dense distribution of the diffraction spots in $\text{ZA} = \langle 100 \rangle_{\text{Al}}$.

Thus, the presence of aggregates with different precipitate morphologies and orientations does not allow separating them according to their shape using $\{100\}_{\text{Al}}$ projections and conventional TEM. The use of the $\{110\}_{\text{Al}}$ projections and a DF-TEM mode with $\vec{g} = 100_{\text{Al}}$ helps to highlight the plate-shaped particles. It is seen in figure 1d that the diffraction spots for the β'' - and β' -Cu phases are weak. The C, Q', θ' and S1 phases have strong diffraction spots in $\langle 110 \rangle_{\text{Al}}$ ZA (figure 1d), and the DF intensity is sufficient to distinguish the plate-shaped particles (marked by b_1 in figure 1b) due to their edge-on orientations. Previous high-resolution TEM analysis of the same alloy [1,2] showed that the C-phase appears as small fragments being predominantly inter-grown with other phases. It makes us conclude that bright 'rectangles' in the DF images are mostly θ' plates. The "disappearance" of rod-shaped particles in DF images using $\vec{g} = 100_{\text{Al}}$ are seen in figure 1b. This is due to the rods which are 45° -tilted to the $\{110\}_{\text{Al}}$ projection plane (marked as b_2) and the rods lying in the projection plane (b_3), which become dark in the respective DF images.

A joint analysis of $\{100\}_{\text{Al}}$ and $\{110\}_{\text{Al}}$ projections allows us to get all information about the precipitate parameters. In the case of the $\{110\}_{\text{Al}}$ projection, one third of the $\{100\}_{\text{Al}}$ plates of the laths/plates are seen to measure the plate diameter (D) and thickness (t). The number density of the plates can be estimated as

$$N_{V_p} = N_p (A_S (\varphi + D))^{-1} + 2N_p A_S^{-0.5} \quad (1)$$

where N_p is the number of the counted plates in each TEM image (the total number of plates counted (n) was 241 in all TEM images), φ is the foil thickness and A_S is the respective TEM image area. This equation was developed using the methodology described in [5] and takes the precipitate orientation features in the respective projections into account. It is assumed that the number of the plates/laths crossed by the projection plane and seeing in the DF images taken along the $\langle 110 \rangle_{\text{Al}}$ ZA is higher than the plates/laths 45° -tilted to the projection plane. In the case of $\{100\}_{\text{Al}}$ projections, one third and two third of the $\langle 100 \rangle_{\text{Al}}$ rods are seen as 'dots' and 'rectangles', respectively. An equivalent circular rod diameter can be calculated as $D_{req} = 2(S_r/\pi)^{0.5}$, where S_r is the rod cross-section area. The total number of cross-sections counted (n) was 1023 in all TEM images. The average length (L) of the elongated 'rectangles' can also be measured representing a common parameter for the rods and plates due to similar visibility for both precipitate types in the $\{100\}_{\text{Al}}$ projection. The L value is required to put into equation (1) with N_r (the total number of the counted rod cross-sections) instead of D and N_p , respectively, to estimate the number density of the rods (N_{V_r}). In this case, the equation (1) takes into account that the number of the rods crossed by projection plane and seeing in the BF TEM images taken along $\langle 100 \rangle_{\text{Al}}$ ZA is higher than the rods parallel to the projection plane (orthogonal to the $\langle 100 \rangle_{\text{Al}}$ ZA). An average L value was calculated using 1286 measurements in all TEM images. An average rod true length can be estimated using statistical joint analysis of length/diameter distributions for the rods and plates (L) obtained from the $\{100\}_{\text{Al}}$ projection and the single distribution of the plates (D) obtained from the $\{110\}_{\text{Al}}$ projection as

$$L_r = (N_{V_p} + N_{V_r})^{-1} \sum_{i=1}^n L_i (N_i - N_{p_i}) \quad (2)$$

where N_{V_p} and N_{V_r} is the number density of the plates and rods, respectively, L_i is the bin width of the 'rectangle' length (L) or plate diameter (D) in the distribution histograms, N_i and N_{p_i} are the number densities of the rods and plates, respectively, in each bin width interval. The total volume fractions, F_V , of the rods and plates within the grain/subgrain can be calculated as

$$F_V = N_V \times f_i \quad (3)$$

where N_V is the number density of the rods (N_{V_r}) or plates (N_{V_p}), f_i is the average volume of the rods and plates approximated as an ideal cylinder ($f_i = \pi(D_{req}/2)^2 L_r$ and $f_i = \pi(D/2)^2 t$ for the rods and

plates, respectively).

All the measured and estimated precipitate parameters in the alloy aged for 96 h are shown in figure 2. During this quantification procedure, the parameters of, at least, one thousand rod cross-sections and ‘rectangles’ in the $\{100\}_{\text{Al}}$ projections and two hundred plate/laths in the $\{110\}_{\text{Al}}$ projections have been measured. It is seen that the geometrical size distributions of precipitates are quite similar for both rod- and plate-shaped precipitates, but the number density of the former is one order higher than for the latter. In general, our quantitative analysis shows that similar volume fraction values were reached for both precipitate groups (rods and plates) in the alloy aged at 170 °C for 96 h. A validation for all parameters is needed by comparing with the numbers obtained using other techniques, and this is the aim of future work.

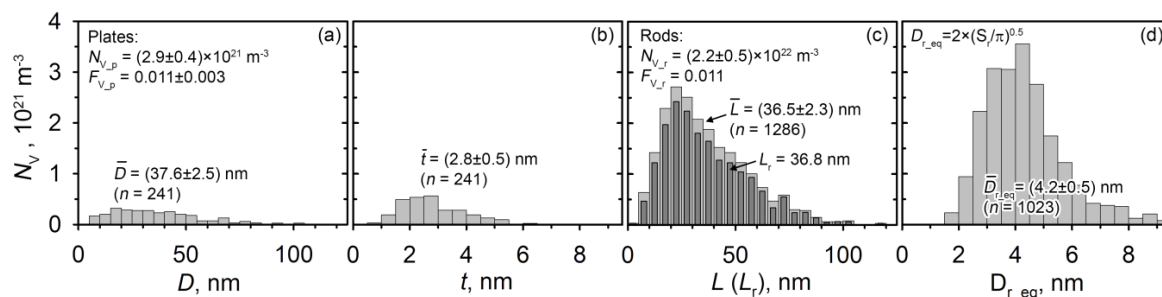


Figure 2. The plate diameter (a) and thickness (b) as well as true rod length (c) and equivalent circular diameter (d) distributions in the aged at 170°C for 96 h. $N_{V,p}$, $N_{V,r}$, \bar{D} , \bar{t} , \bar{L} (‘rectangle’ length in $\{100\}_{\text{Al}}$ projection), $\bar{D}_{r,eq}$ and $F_{V,p}$ (for the plates) were averaged using at least three TEM images in respective projections.

Conclusions

By combining tilting and DF imaging, it has been possible, using conventional TEM, to determine precipitate parameters and separate $\langle 100 \rangle_{\text{Al}}$ rods and $\{100\}_{\text{Al}}$ plates/laths in the Al-Cu-Mg-Si alloy aged at 170 °C for 96 h. It was found that the most obvious feature of precipitation behavior in this aged alloy is that the number density of rod-shaped precipitates is ten times higher than for the plates, despite the fact that they have similar volume fractions.

Acknowledgements

This work was financially supported by the Ministry of Science and Higher Education and Council on Grant No. 075-15-2019-994 and the Faculty of Natural Sciences at the Norwegian University of Science and Technology (NTNU), Project No. 81617879 using the NORTEM infrastructure (grant number NFR197405) at the TEM Gemini Centre.

References

- [1] Gazizov M, Marioara CD, Friis J, Wenner S, Holmestad R and Kaibyshev R 2019 *Mater. Sci. Eng. A* **767** 138369
- [2] Gazizov M, Marioara CD, Friis J, Wenner S, Holmestad R and Kaibyshev R 2020 *J. Alloy. Compd.* **826** 153977
- [3] Dorin T, Deschamps A, De Geuser F and Sigli C 2014 *Acta Mater.* **75** 134
- [4] Sunde JK, Marioara CD, van Helvoort ATJ and Holmestad R 2018 *Mater. Char.* **142** 458
- [5] Nie J-F and Muddle BC 2008 *Acta Mater.* **56** 3490
- [6] Gazizov M and Kaibyshev R 2017 *Mater. Sci. Eng. A* **702** 29
- [7] Andersen SJ 1995 *Metall. Mater. Trans.* **26A** 1931
- [8] Yang W, Wang M, Yanlin J and Zhang R 2011 *Metall. Mater. Trans.* **42A** 2917
- [9] Wang SC and Starink MJ 2005 *Inter. Mater. Rev.* **50(4)** 193